


# Availability Estimation of Optical Network Links Using Multilevel Bayesian Modeling

Filippos Christou 

*Institute of Communication Networks and Computer Engineering (IKR)*

*University of Stuttgart*

Stuttgart, Germany

filippos.christou@ikr.uni-stuttgart.de

**Abstract**—Estimating availability in transport networks is essential to successfully provision connectivity services under various requirements. As modern Service Level Agreements (SLAs) are becoming more demanding, it is crucial to estimate the true availability of an end-to-end path as soon and reliably as possible. Network operators might have expert knowledge regarding the theoretical availability of the network components, or they might have some measured data to infer such information. However, in either case, the true steady-state availability is unknown and must be inferred as a combination of the above. Traditionally, the estimation of Quality of Service (QoS) metrics, like availability, is done by producing a scalar value as an approximation. This can often be misleading and an oversimplification. In this paper, we build a multilevel Bayesian model that provides a probabilistic estimate of all network links' availability by exploiting expert knowledge and the underlying data. The value of this methodology is greater for scenarios with scarce data, where the inference quality demonstrates remarkable stability regardless of the randomness of the incoming data. We demonstrate the effectiveness of our approach through simulation experiments and compare our results with the empirical interval availability. Our work has important implications for the design and management of optical networks since it constitutes a valuable tool that provides accurate availability estimations, which can be used for sophisticated decision-making.

**Index Terms**—availability, modeling, Bayesian, optical networks

## I. INTRODUCTION

Modern networking introduces new challenges with ever more demanding requirements. The emergence of 5G/6G technologies may provide an answer for such high-end services, but the optical network section must properly support them. The network operators must adjust their configuration to align with the promised Quality of Service (QoS) metrics of the Service Level Agreement (SLA). One of the most popular QoS metrics in an SLA is availability. The availability is a way to specify the uptime of a system, and it is typically measured as the percentage of time that the system is available and usable. Network operators might often be interested in steady-state availability, which describes the availability of a system in the long run. They can use this information to make optimized decisions to implement network services of different availability requirements without overprovisioning and wasting precious resources.

There has generally been much research regarding network availability. However, the estimation of the true steady-state

availability has often been considered equivalent to the empirical interval availability [1]. The empirical interval availability is the measured availability that the system experiences in a specific time interval. We question this method, which we find inappropriate for scarce events, as is the nature of optical fiber faults measured over a limited time. We propose an alternative approach to estimate the steady-state availability more reliably using multilevel Bayesian modeling.

Bayesian modeling [2] has its roots in Bayesian statistics. It provides a technique to incorporate expert knowledge and measured data into a model and describe the estimation of the parameters with probability distributions. It has recently gained much usability due to advancements in computing resources and the emergence of Probabilistic Programming Languages (PPLs). PPLs automatically infer the estimated parameters by commonly using Markov Chain Monte Carlo (MCMC) sampling.

Following, we mention a non-exhaustive list of the most important works related to this paper. [3] defines an availability model for multiple types of IP-optical network equipment, including fibers, and uses a triplet of scalar values to represent different availability measures. The authors in [4] describe methods for calculating the overall network reliability, given that the link failure probability is already known. In [1], a methodology is developed to estimate the interval availability for protected connections, and a summary is given about previous works on availability estimation. [5] constructs a two-level availability model for software-defined backbone networks and compares the network availability with that of traditional IP-routed networks.

This paper differentiates from all previous work in that it is the first to use Bayesian modeling to estimate the steady-state availability of the network fiber links. We accomplish this by building a statistical model of the downtimes and uptimes of a link and feeding into that model measured data retrieved over a limited time window. Our methodology is independent of any routing or protection mechanisms. Our model has several advantages over using the empirical interval availability, which serves as our baseline, like accuracy, reliability, uncertainty estimation.

The paper is structured as follows. Section II explains the basics of Bayesian modeling and formulates the model for estimating the availability of all network links. Section III evaluates the model and compares the estimations with the empirical interval availability. In Section IV, we offer the concluding remarks.

This work has been performed in the framework of the CELTIC-NEXT EUREKA project AI-NET-ANTILLAS (Project ID C2019/3-3), and it is partly funded by the German BMBF (Project ID 16KIS1312).

## II. MODELING

In this Section, we will develop a Bayesian model for availability estimation in optical networks. Firstly in Section II-A, we will revisit the basics of Bayesian modeling. In Section II-B, we will formulate the multilevel Bayesian model, and in Section II-C, we will conduct the prior analysis.

### A. Bayesian Modeling Basics

Bayesian modeling is based on Bayes' theorem.

$$P(\theta|y) = \frac{P(y|\theta) \cdot P(\theta)}{P(y)} \quad (1)$$

$y$  is the evidence (i.e., data) observed in an experiment, and  $\theta$  are the parameters we want to estimate.  $P(\theta|y)$  is the *posterior* distribution, which expresses the probability density function (PDF) of the parameters after consuming the evidence  $y$ .  $P(y|\theta)$  is the *likelihood* of the model, which expresses the PDF of the data given the parameters.  $P(\theta)$  is the *prior* distribution of the initial beliefs (expert knowledge) and represents the PDF of the parameters before considering the data. The denominator  $P(y)$  is known as *marginal likelihood*, and although it can be troublesome to calculate, it can often be ignored, especially for the MCMC inference methods.

To formulate a Bayesian model, we need to specify the likelihood  $P(y|\theta)$  and the prior  $P(\theta)$ . Then given some data  $y$  generated by the investigated stochastic process, we can infer the posterior  $P(\theta|y)$ . Altogether, the posterior incorporates modeling assumptions through the likelihood, expert knowledge beliefs through the prior, and the influence of the data  $y$  due to the inference. There are numerous methodologies to conduct Bayesian inference. We use the No-U-Turn Sampler (NUTS) [6], a state-of-the-art variant belonging to the MCMC algorithmic family. MCMC algorithms do not produce a closed-form solution. Instead, they search the parameter space and return a chain of values that are representative samples of the posterior distribution.

A powerful technique of Bayesian modeling is grouping observed data together by analyzing hierarchical or nested stochastic processes. This gives birth to multilevel modeling. As the name might suggest, a parameter  $\theta$  may not be exclusively dependent on a prior distribution  $P(\theta)$  but instead on  $P(\theta; k)$ , where  $k$  is an additional parameter, which is also a Random Variable (RV) with another PDF  $P(k)$ . This way, multiple modeling levels are created.

### B. Availability Multilevel Bayesian Model

In this subsection, we will derive a Bayesian model for the steady-state availability (from now on, just *availability*)

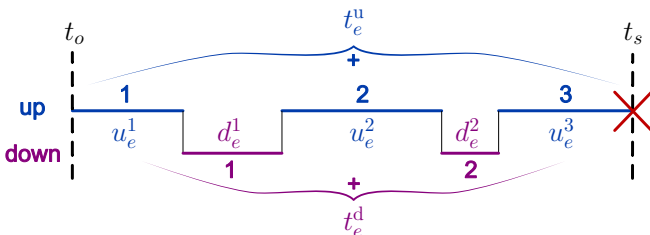


Fig. 1. Uptimes and downtimes representation in a link  $e$ .

estimation of network links. Let  $G(V, E)$  be the graph of a network with a set of nodes  $V$  and a set of undirected edges (i.e. links)  $E$  with link length  $l_e \forall e \in E$ . Let  $a_e$  be the true availability of link  $e \in E$  we want to estimate. Let  $f_e$  be the true Mean Time To Failure (MTTF) of link  $e$  and  $r_e$  the true Mean Time To Repair (MTTR). The availability is known to be

$$a_e = \frac{f_e}{f_e + r_e} \quad (2)$$

While operating the network, we observe a time series of uptime and downtime measurements of a link  $e$ . Our measurements span a limited time window between  $t_o$  and  $t_s$ . Let  $U_e = \{u_e^1, u_e^2, \dots\}$  be the set of experienced uptimes of link  $e$  in chronological order, and  $D_e = \{d_e^1, d_e^2, \dots\}$  be the set of experienced downtimes between them. An illustration of these quantities is given in Fig. 1. Let  $U$  be the superset containing all  $U_e \forall e \in E$  and  $D$  be the superset containing all  $D_e \forall e \in E$ .  $U$  and  $D$  are the data of our process. The empirical overall uptime and downtime are given by (3) and (4) correspondingly.

$$t_e^u = \sum U_e = \sum_i u_e^i \quad (3)$$

$$t_e^d = \sum D_e = \sum_i d_e^i \quad (4)$$

It holds that  $t_s - t_o = t_e^u + t_e^d \forall e \in E$ . Based on these measurements, we can calculate the empirical interval availability  $a_e^{\text{emp}}$  (from now on, just *interval availability*) of link  $e$ .

$$a_e^{\text{emp}} = \frac{t_e^u}{t_e^u + t_e^d} \quad (5)$$

We can also calculate the empirical MTTF  $f_e^{\text{emp}}$  and MTTR  $r_e^{\text{emp}}$ . However, we need to be cautious because the last measurement of either  $U_e$  or  $D_e$  has been interrupted, and we must not take it into account for this calculation. In other words, either  $u_e^{|\cdot|}$  or  $d_e^{|\cdot|}$  must be discarded  $\forall e \in E$ , where  $|\cdot|$  denotes the cardinality of the enclosed set. For example, in Fig. 1,  $u_e^3$  must be ignored as it is interrupted due to the end of the measurement period. We assume that our measurements start together with the network equipment provisioning in a working (up) state, so we do not need to do the same for  $u_e^1$  or  $d_e^1$ . Let  $U'_e$  and  $D'_e$  denote these meta-processed data sets where the last disrupted measurement has been discarded, and  $U', D'$  be the supersets  $\forall e \in E$ . Then,  $f_e^{\text{emp}}$  and  $r_e^{\text{emp}}$  can be derived from (6) and (7).

$$f_e^{\text{emp}} = \frac{\sum U'_e}{|U'_e|} \quad (6)$$

$$r_e^{\text{emp}} = \frac{\sum D'_e}{|D'_e|} \quad (7)$$

To construct the statistical model, we first assume that the link uptimes and downtimes follow an exponential distribution.

$$\text{PDF}_{\text{exponential}}(x; \mu) = \frac{1}{\mu} e^{-\frac{1}{\mu}x} \quad (8)$$

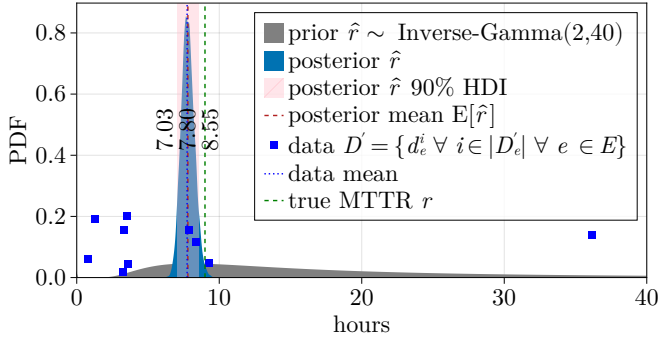


Fig. 2. Prior and posterior distributions for estimated MTTR  $\hat{r}$ .

$$u_e^i \sim \text{Exponential}(\hat{f}_e) \quad \forall i \in |U_e^i| \quad \forall e \in E \quad (9)$$

$$d_e^i \sim \text{Exponential}(\hat{r}_e) \quad \forall i \in |D_e^i| \quad \forall e \in E \quad (10)$$

where  $\sim$  signifies that the Left-Hand Side (LHS) follows the distribution on the Right-Hand Side (RHS). The LHS can be either data, e. g., like (9) and (10), or an RV. The variables  $\hat{f}_e, \hat{r}_e$  are RVs denoting the estimation of  $f_e, r_e$ .

The estimated MTTF  $\hat{f}_e$  might be different for every link, but we considered the estimated MTTR  $\hat{r}_e$  to be the same for all links  $\hat{r} = \hat{r}_e \quad \forall e \in E$ . Now we need to find a prior distribution for the parameters  $\hat{f}_e$  and  $\hat{r}$ . A common prior distribution for an exponential likelihood model is the gamma distribution, as they also form a conjugate prior pair. However, we have parametrized the exponential distribution (8) with the mean value  $\mu$ , which is reciprocal to the rate parameter  $\lambda$ , i. e.,  $\mu = 1/\lambda$ . And if we model  $\lambda$  to follow a gamma distribution, then  $\mu$  should follow an inverse-gamma distribution.

$$\text{PDF}_{\text{inverse-gamma}}(x; \alpha, \beta) = \frac{\beta^\alpha x^{-\alpha-1}}{\Gamma(\alpha)} e^{-\beta/x} \quad (11)$$

The prior distributions for (9) and (10) are

$$\hat{f}_e \sim \text{Inverse-Gamma}(\alpha_e^f, \beta_e^f) \quad \forall e \in E \quad (12)$$

$$\hat{r} \sim \text{Inverse-Gamma}(\alpha^r, \beta^r) \quad (13)$$

We need to specify values for  $\alpha_e^f, \beta_e^f, \alpha^r$ , and  $\beta^r$  based on expert knowledge prior beliefs. To demonstrate flexibility, we consider weakly informative priors covering the parameter space's plausible values. However, stricter priors could be provided depending on the theoretical background or expertise. For the estimated MTTR,  $\hat{r}$ , we consider a prior distribution with  $\alpha^r = 2$ ,  $\beta^r = 40$ , i. e., Inverse-Gamma(2, 40) as shown in Fig. 2.

To model  $\alpha_e^f$  and  $\beta_e^f$ , we will leverage the power of multilevel modeling, meaning we will not need to specify a prior directly as we did for  $\hat{r}$ . We know that  $\hat{f}_e$  should depend on the link length  $l_e$ , and the larger the link length, the more probable it is for the link to fail. Literature [3] suggests that the relationship of failures over link length follows a reciprocal function, which is also the consideration of this model.

$$\tilde{f}(l_e; k, s, h) = k + \frac{s}{l_e - h} \quad (14)$$

In function (14), the LHS  $\tilde{f}(l_e)$  is the suggested MTTF for a link with length  $l_e$ . Now we need to bind  $\tilde{f}(l_e)$  of (14) to the prior parameters  $\alpha_e^f, \beta_e^f$  of (12). We want to make (14) the mean of the inverse-gamma distribution. Thus, we set one of the prior parameters of the inverse-gamma distribution to be fixed, and we model the other parameter such that we get an overall distribution with the desired mean. We keep the prior shape parameter  $\alpha$  of the inverse-gamma distribution in (11) fixed and set the scale parameter as  $\beta = m \cdot (\alpha - 1)$ . The LHS is the scale parameter  $\beta$  that we must choose to achieve the desired mean value  $m$  in an inverse-gamma distribution with shape parameter  $\alpha$ . The desired mean value  $m$  is taken from (14), and the shape value  $\alpha_e^f$  is initiated with a prior of  $\alpha_e^f = 10 \quad \forall e \in E$ .

$$\beta_e^f = \tilde{f}(l_e; k, s, h) \cdot (\alpha_e^f - 1) \quad (15)$$

We note that (14) will be forced to be the mean of (12) as a prior, but depending on the data during inference, (12) might deviate.

We also need to specify the parameters  $k, s$ , and  $h$  of (14). Since it makes sense that  $\lim_{l_e \rightarrow 0} \tilde{f}(l_e) = \infty$ , we fix the parameter  $h = 0$ . We want to keep both  $k$  and  $s$  positive with a long tail on the right side, so we model them using a Gamma distribution and the following priors.

$$\text{PDF}_{\text{gamma}}(x; \alpha, \theta) = \frac{x^{\alpha-1} e^{-x/\theta}}{\Gamma(\alpha)\theta^\alpha} \quad (16)$$

$$k \sim \text{Gamma}(k_\alpha, k_\theta) \sim \text{Gamma}(0.8, 9) \quad (17)$$

$$s \sim \text{Gamma}(s_\alpha, s_\theta) \sim \text{Gamma}(2, 155) \quad (18)$$

The choice of the prior values is not definite and will be analyzed in Section II-C. The parameter  $\beta_e^f$  of (12) is now also an RV since it depends through (14) and (15) on the RVs  $k$  and  $s$ .

Until now, we managed to use all information inside  $U_e^i$  and  $D_e^i$ . However, we still have not used the interrupted last measurement  $u_e^{|U_e^i|}$  or  $d_e^{|D_e^i|}$ . For scarce data situations, it is even more important to incorporate them into our model and take advantage of this information. To incorporate this evidence, we know that an RV that counts events following an exponential inter-arrival time distribution is a Poisson distribution.

$$\text{PDF}_{\text{Poisson}}(x; \lambda) = \frac{\lambda^x e^{-\lambda}}{x!} \quad (19)$$

The average rate of occurrence  $\lambda$  is equal to the total time of the experiment divided by the mean of the underlying exponential distribution. With this in mind, we model the counts of uptime and downtime events.

$$|U_e^i| \sim \text{Poisson}\left(\frac{t_e^u}{\hat{f}_e}\right) \quad \forall e \in E \quad (20)$$

$$\sum_e |D_e^i| \sim \text{Poisson}\left(\frac{\sum_e t_e^d}{\hat{r}}\right) \quad (21)$$

The total count of failures in a link  $e$  equals the count of uptime intervals  $|\{u_e^1, u_e^2, \dots\}| = |U_e^i|$ . The total time of this Poisson experiment is  $t_e^u$  since only when the link is up can it go down. The formulation is similar for the total count of repairs, only that this time we aggregate together all links. This is

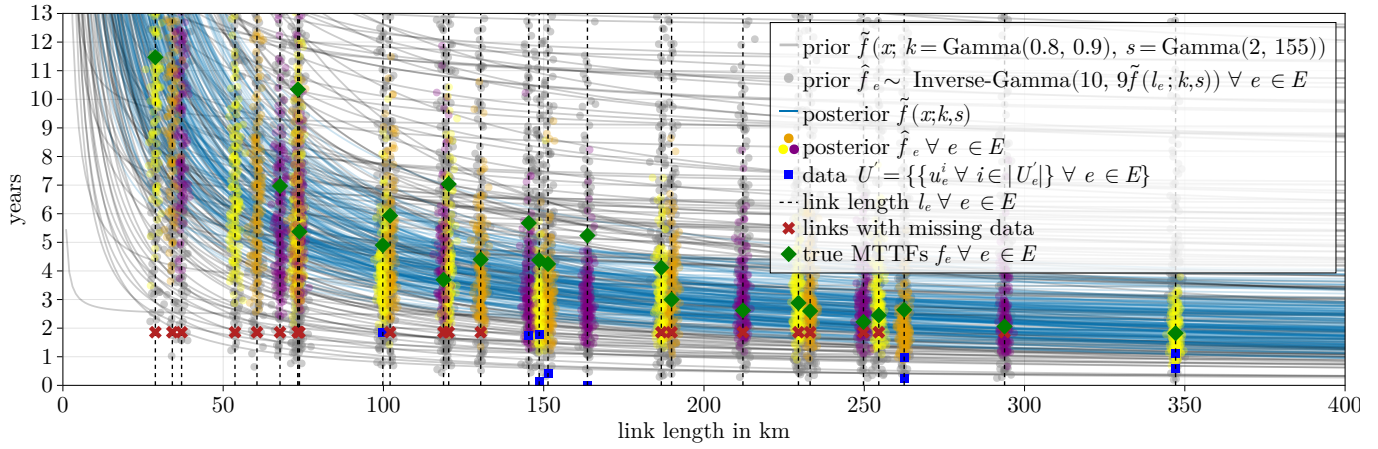
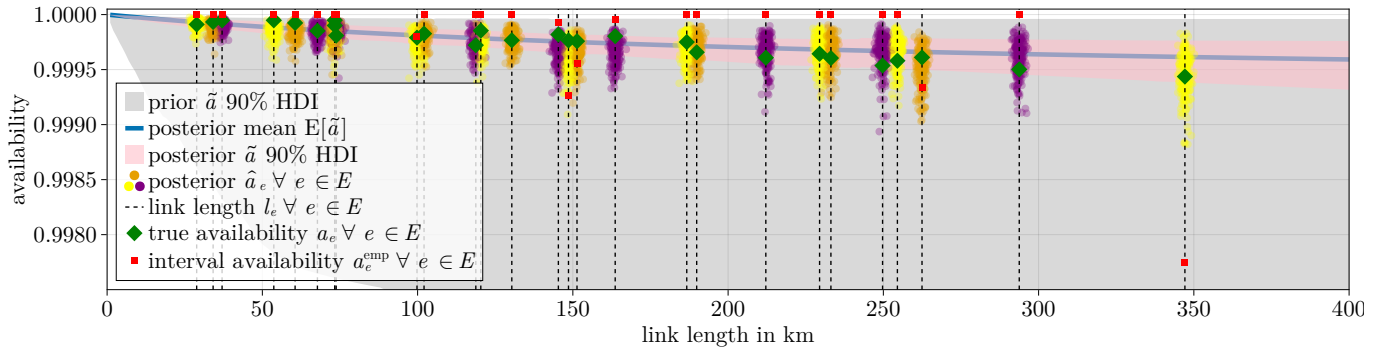

 (a) Prior and posterior distributions for estimated MTTF  $\hat{f}_e$  and  $\tilde{f}$ .

 (b) Estimated availabilities  $\hat{a}_e$  and  $\tilde{a}$ .

Fig. 3. Estimation of MTTFs and availabilities.

possible because the sum of independent Poisson distributions  $X_i \sim \text{Poisson}(\lambda_i)$  is still Poisson  $\sum_i X_i \sim \text{Poisson}(\sum_i \lambda_i)$ . We do this because we expect scarce events, and some links never fail during our measurements. In this case, we would have  $t_e^d = 0$ , giving an illegal rate for the Poisson distribution. Equation (21) handles it by aggregating all downtimes together. Overall (20) and (21) incorporate the interrupted last measurement using the  $t_e^u$  and  $t_e^d$  evidence.

Following, we repeat the complete Bayesian model.

$$u_e^i \sim \text{Exponential}(\hat{f}_e) \quad \forall i \in |U'_e| \quad \forall e \in E \quad (22a)$$

$$d_e^i \sim \text{Exponential}(\hat{r}) \quad \forall i \in |D'_e| \quad \forall e \in E \quad (22b)$$

$$|U'_e| \sim \text{Poisson}\left(\frac{t_e^u}{\hat{f}_e}\right) \quad \forall e \in E \quad (22c)$$

$$\sum_e |D'_e| \sim \text{Poisson}\left(\frac{\sum_e t_e^d}{\hat{r}}\right) \quad (22d)$$

$$\hat{f}_e \sim \text{Inverse-Gamma}(10, \beta_e^f) \quad \forall e \in E \quad (22e)$$

$$\hat{r} \sim \text{Inverse-Gamma}(2, 40) \quad (22f)$$

$$\tilde{f}(l_e; k, s) = k + \frac{s}{l_e} \quad (22g)$$

$$k \sim \text{Gamma}(0.8, 9) \quad (22h)$$

$$s \sim \text{Gamma}(2, 155) \quad (22i)$$

$$\beta_e^f = 9\tilde{f}(l_e; k, s) \quad \forall e \in E \quad (22j)$$

The (22a–22d) are part of the model's likelihood since all LHSs are data observations. The priors are tuned for up/downtimes measured in hours and link distances in kilometers (km).

### C. Prior Analysis

During prior analysis, we will confirm the validity of the selected priors. Fig. 2 shows with gray the prior MTTR  $\hat{r}$  distribution. The Inverse-Gamma(2, 40) prior is weakly informative but still introduces the desired constraints. The inverse-gamma distribution allows only positive values, which are valid for our use. Also, the choice of the parameters does not encourage MTTRs close to 0 hours and does not exclude very high MTTRs because of the long tail. We remind that the prior distribution models the mean parameter for an exponential distribution and is not the likelihood of the data itself.

Now we analyze the choice of the priors  $\alpha_e^f = 10$  from (22e) and the priors from (22h–22j). This time plotting each prior distribution distinctively will not give us significant insight. The RVs of interest are  $\hat{f}_e$  and  $\tilde{f}$  because they reveal essential information about the system. The first reveals the estimated MTTF per link, and the second the influence of the link length. Both involve operations between several RVs, and finding a closed-form distribution is hard or impossible. Therefore, we visualize each by sampling all involved prior distributions and calculating  $\hat{f}_e$  and  $\tilde{f}$  for each sample. Fig. 3a demonstrates



the sampled priors for  $\tilde{f}$  and  $\hat{f}_e$  with gray lines and scattered gray circles correspondingly. Every gray line is a sample of the priors of  $\tilde{f}$  representing a possible reciprocal relationship. The numerous widely spread reciprocal lines indicate that the underlying priors hardly exclude any possibilities. Similarly, the gray circles, which are priors for  $\hat{f}_e$ , are quite wide since they span from 0 to 13 years and beyond. Although we kept our priors weakly informative on purpose, in order not to introduce any bias into the model, network operators with more exact knowledge can leverage stricter priors to have more precise inference. With multilevel modeling, we build an overall reciprocal relationship (22g–22j) for all links and their dependence on link length. Moreover, each network link is individually modeled (22e) to obey the overall reciprocal relationship but can also differentiate itself from the group.

### III. EVALUATION

We evaluate our model using simulative data and compare the results with the interval availability. We generated data for a two-year timeframe for a German topology [7] with two additional links to France based on [8]. The data generation was done using a reciprocal relationship between the link length and failure events, according to [3]. We added an extra layer of randomness with a positive truncated normal distribution to demonstrate some generalization abilities of the Bayesian model. All up/downtime data were generated with an exponential distribution, and we used the same PDF for all link downtimes.

#### A. Inference

First, we normalized our data as we experienced that it facilitated the inference. We normalized all uptimes  $U$  by dividing them with their standard deviation. We employed the NUTS algorithm with 30 parallel chains, each with 3000 samples using the Turing [9] PPL. We inspected the inference quality and concluded that the metrics satisfy guidelines like [10]. The  $\hat{R}$  convergence metric and the potential scale reduction factor (PSRF) were close to  $1 \pm 0.1\%$ , and the effective sample sizes (ESSs) of the parameters were around 10000.

The posterior for  $\hat{r}$  is visible with blue in Fig. 2. The transition from the gray prior to the blue posterior was exclusively due to the blue square data points  $D'$ . With a distribution instead of a scalar value as an estimation, we can assess uncertainty. We could narrow it down to a scalar value by,

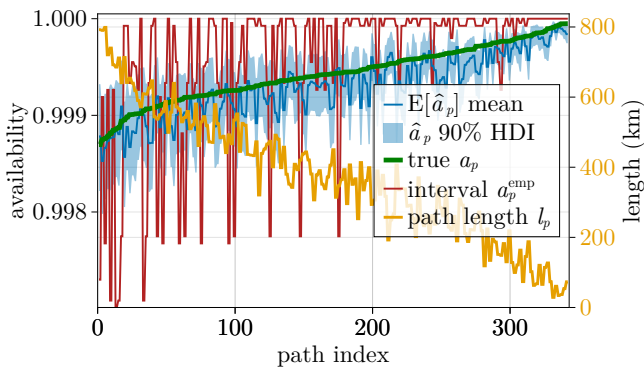


Fig. 4. Path availability estimation  $\hat{a}_p$ .

e. g., taking the expected value of the posterior distribution (in the MCMC case, it is the average of all the samples), which is equal to 7.80 hours. Similarly, we can calculate Highest Density Intervals (HDIs), e. g., yielding that the model is 90 % confident that the true MTTR  $r$  lies within (7.03, 8.55). In this simulation, the data mean coincides more or less with the posterior mean, and the true MTTR  $r$  is slightly higher at 9 hours.

The posteriors  $\tilde{f}$  and  $\hat{f}_e$  are visible in Fig. 3a. The blue lines denote the posterior for  $\tilde{f}$  by updating the  $k$  and  $s$  parameters of the continuous reciprocal relationship (22g). The colorful scattered circles are the posteriors of  $\hat{f}_e$ , discrete for each link. The concentration of the lines or the scattered circles denotes the probability mass. The colors of the circles are different to visually separate consecutive links. Most links have never failed and thus have no  $U'_e$  data. This is noted with the red cross positioned at the time point where the measurement stopped. This information is vital for a good inference and should not be ignored. That is why we insisted on incorporating this knowledge using the Poisson distribution in (22c) and (22d). Despite the scarcity of the data, we see that the inference is satisfactory and can approximate the true values of the green rhombuses. Namely, 24 out of 28 true MTTFs are contained within the 90 % HDI, with an average standard deviation of 2.1 years against the prior standard deviation of 7.5 years. This time, the data mean cannot reach the quality of estimations we achieve with the model. Additionally, we can detect how some links deviate from the reciprocal relationship, like the orange  $\hat{f}_e$  around 262 km, which has the probability mass lower or equal to the purple one at 293 km, thus, going against the reciprocal relationship. The inference will improve with more data, suggesting that this methodology is scalable.

#### B. Availability Estimation

To calculate the inferred availability, we use (2)

$$\hat{a}_e = \frac{\hat{f}_e}{\hat{f}_e + \hat{r}} \quad \forall e \in E \quad (23)$$

We calculate the posterior PDF of (23) using the chain samples from the inference. Fig. 3b shows all link availability estimates. Observe that the interval availability  $a_e^{\text{emp}}$ , illustrated with red squares, is almost always exactly 1 because most links never failed. Of course, such an overestimation of the availability is wrong and unrealistic; an availability of 1 is known to be impossible. The continuous availability estimation  $\tilde{a}$  is calculated using  $\tilde{f}$  instead of  $\hat{f}_e$  in (23). The gray band shows the 90 % HDI of the prior availability  $\tilde{a}$ , which covers a big portion of the parameter space. After inference, the posterior  $\tilde{a}$  90 % HDI is significantly reduced and is much more focused, as appointed by the pink band. The model estimations look more realistic as an availability of 1 is excluded. Additionally, the model estimations have smaller error margins and provide useful uncertainty assessments. We calculated that the expected values of the posterior link availabilities  $E[\hat{a}_e]$  have on average 78 % lower error estimating the true availability with respect to the interval availabilities. Furthermore, having a continuous model of the link availabilities depending on the distance, we

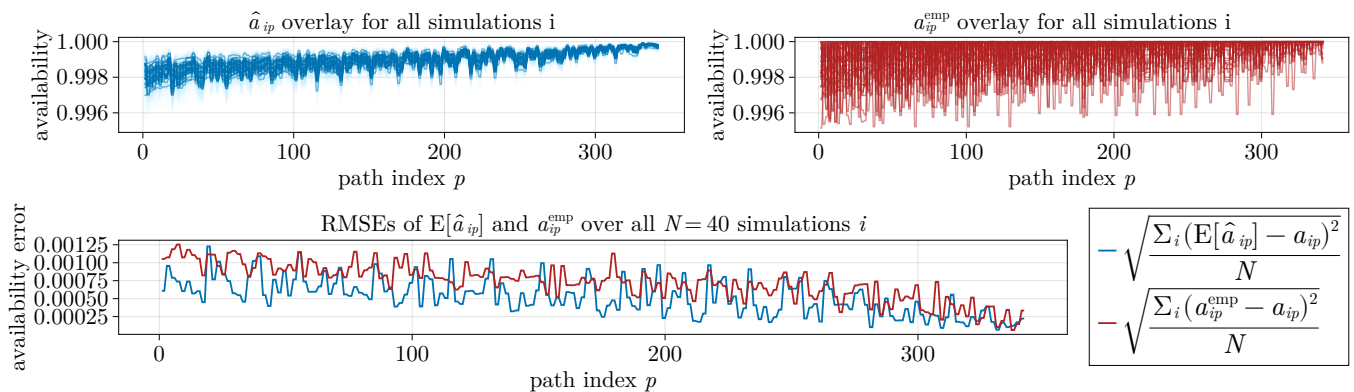


Fig. 5. Comparison between the posterior expected estimations  $E[\hat{a}_p]$  and interval path availabilities  $a_p^{emp}$ . Up, an overlay of multiple curves similar to Fig. 4 over different seeded simulations  $i$ . Down, the RMSE for each path  $p$  over all different seeded simulations  $i$ .

can easily extrapolate a new availability for hypothetical new links, which could be useful for network dimensioning.

We can also calculate the posterior availability  $\hat{a}_p$  for a path  $p$  by multiplying the availabilities (i. e. the samples) of all the participating links. Fig. 4 illustrates all the end-to-end path availabilities. The baseline is the interval path availability  $a_p^{emp}$  which factors in the empirical end-to-end path uptimes and downtimes. We observe the erratic behavior of  $a_p^{emp}$  and the unreliable estimations. On the contrary, the model estimations  $\hat{a}_p$  are more consistent and mostly include the true availability value inside the 90% HDI. We also observe that the model slightly underestimates the path availabilities. This is because the long tails of the gamma and inverse-gamma distributions grant the model estimations a skewed character. For a few data, this effect is desirable, and for more data, it diminishes. We see that the  $\hat{a}_p$  uncertainty is greater for longer paths. This is because longer routes contain more links, and with every link availability multiplication, the uncertainty propagates and accumulates. As more data become available due to a longer measurement period,  $a_p^{emp}$  and  $\hat{a}_p$  will begin to look more alike.

Finally, we conducted the above simulation 40 times using different seeds to generate different up/downtime measurement data. We compared  $a_p^{emp}$  and  $\hat{a}_{ip}$  for different simulations  $i$  in Fig. 5. On the upper left plot, we notice the consistency of the estimates for different data inputs. On the upper right plot, the interval path availabilities are spontaneous and with high variance. We do not average the curves as this would undisputably favor the interval availabilities due to the law of large numbers. Our model might make consistently good estimations, but it also consistently makes some bad ones; it can mainly be improved with more data or more informative priors. Given that the network operator cannot artificially generate realistic data or conduct the experiment several times (since the interest lies in the real infrastructure), our model gives a more reliable one-shot estimation. It is fair to compare the  $\hat{a}_p$  and  $a_p^{emp}$  using the Root Mean Square Error (RMSE) over all simulations with respect to the true path availabilities. Although the posterior  $\hat{a}_p$  is a distribution, we choose a scalar value for the comparison, e. g., the expected value  $E[\hat{a}_p]$ . These results are shown in the lower plot of Fig. 5. After averaging over all paths, the model estimations present a 52% lower error.

#### IV. CONCLUSIONS

Our study demonstrates the effectiveness of using Bayesian multilevel modeling for estimating the availability of links and paths in optical networks. We found that this approach significantly improves upon simply using the empirical interval availability. Our results suggest that this method can be a valuable tool for network designers and operators seeking to improve the availability estimations of their networks and who also want to account for uncertainty. Our model is especially helpful for scenarios with scarce data and can also scale well given more. Future work can involve further additions to the model by including node availabilities and other QoS metrics.

#### REFERENCES

- [1] D. A. Mello, H. Waldman, and G. S. Quitério, "Interval availability estimation for protected connections in optical networks," *Computer Networks*, vol. 55, no. 1, pp. 193–204, 2011.
- [2] R. van de Schoot, S. Depaoli, R. King, B. Kramer, K. Märtens, M. G. Tadesse, M. Vannucci, A. Gelman, D. Veen, J. Willemsen, and C. Yau, "Bayesian statistics and modelling," *Nature Reviews Methods Primers*, vol. 1, no. 1, p. 1, Jan 2021. [Online]. Available: <https://doi.org/10.1038/s43586-020-00001-2>
- [3] S. Verbrugge, D. Colle, P. Demeester, R. Huelsermann, and M. Jaeger, "General availability model for multilayer transport networks," in *DRCN 2005. Proceedings. 5th International Workshop on Design of Reliable Communication Networks, 2005.*, 2005, pp. 8 pp.–.
- [4] G. Booker, A. Sprintson, C. Singh, and S. Guikema, "Efficient availability evaluation for transport backbone networks," in *2008 International Conference on Optical Network Design and Modeling*, 2008, pp. 1–6.
- [5] G. Nencioni, B. E. Helvik, A. J. Gonzalez, P. E. Heegaard, and A. Kamisinski, "Availability modelling of software-defined backbone networks," in *46th Annual IEEE/IFIP International Conference on Dependable Systems and Networks Workshop*, 2016, pp. 105–112.
- [6] M. D. Hoffman and A. Gelman, "The no-u-turn sampler: Adaptively setting path lengths in hamiltonian monte carlo," 2011. [Online]. Available: <https://arxiv.org/abs/1111.4246>
- [7] S. Orłowski, R. Wessälly, M. Pioro, and A. Tomaszewski, "Sndlib 1.0—survivable network design library," *Networks*, vol. 55, pp. 276 – 286, 01 2009.
- [8] S. Knight, H. Nguyen, N. Falkner, R. Bowden, and M. Roughan, "The internet topology zoo," *Selected Areas in Communications, IEEE Journal on*, vol. 29, no. 9, pp. 1765 –1775, october 2011.
- [9] H. Ge, K. Xu, and Z. Ghahramani, "Turing: a language for flexible probabilistic inference," in *International Conference on Artificial Intelligence and Statistics, AISTATS 2018, 9-11 April 2018, Playa Blanca, Lanzarote, Canary Islands, Spain*, 2018, pp. 1682–1690.
- [10] J. K. Kruschke, "Bayesian analysis reporting guidelines," *Nature Human Behaviour*, vol. 5, no. 10, pp. 1282–1291, Oct 2021. [Online]. Available: <https://doi.org/10.1038/s41562-021-01177-7>